SINONASAL COMPLEX: RADIOLOGICAL ANATOMY*

Ricardo Pires de Souza[1], Joel Pinheiro de Brito Júnior[2], Olger de Souza Tornin[3], Ademar José de Oliveira Paes Junior[4], Cristiano Ventorim de Barros[5], Felipe Amstalden Trevisan[6], Carlos Neutzling Lehn[7]

Abstract **The aim of this study is to evaluate the sinonasal complex to identify the main findings and to determine the diseases in this area. An accurate analysis of the local extent and tumoral dissemination through computed tomography and magnetic resonance imaging plays a significant role in the therapeutic planning, also affecting the prognosis.**
Keywords: Nasal sinuses; Computed tomography; Magnetic resonance imaging.

Resumo *Complexo nasossinusal: anatomia radiológica.*
Este estudo propõe-se a avaliar o complexo nasossinusal, a fim de identificar os principais achados e determinar as doenças desta área. A análise precisa da extensão local e disseminação tumoral, dada pela tomografia computadorizada e ressonância magnética, desempenha papel importante no planejamento terapêutico, influenciando também o prognóstico.
Unitermos: Nasossinusal; Tomografia computadorizada; Ressonância magnética.

INTRODUCTION

Many times, clinical findings in conditions affecting the nasal cavities and paranasal sinuses may be non-specific so in these cases a radiological evaluation is essential[1,2].

Although plain films may depict alterations resulting from inflammatory diseases in paranasal sinuses, computed tomography (CT), particularly, is a better method for evaluating the nasal cavity, paranasal sinuses and adjacent structures, allowing visualization of ostiomeatal channels and facilitating the perception of this region morphology, a characteristic that has been quite explored in the recent years with the increasing use of endoscopic sinonasal surgical techniques[1–11]. Magnetic resonance imaging (MRI) allows a better visualization of soft tissues than CT, however, bone walls and paranasal sinuses ostia are not appropriately demonstrated[1–3,12–15].

The aim of this study is to describe the nasal cavity and paranasal sinuses anatomy which is essential for diagnosis and therapeutical planning in cases of conditions affecting this region, guaranteeing a better assistance for the patient, and also describes the more frequent anatomical variations in this area[1–3].

SINONASAL COMPLEX ANATOMY AND PHISIOLOGY

Mucociliar function (clearance) – The paranasal sinuses is lined with a pseudostratified ciliary columnar epithelium, the cilia being in constant movement and sweeping the mucinous carpet towards the sinusal ostia[1,2,16]. The flow pattern is specific for each sinus and persists even in the presence of alternative openings[1,2,8,9]. This is clearly observed in the maxillary sinus where the mucosal flow is drained into the primary ostium and then is transported through the ethmoid infundibulum towards the semilunar hiatus and after towards the middle meatus. Through the middle meatus, maxillary, ethmoidal and frontal sinuses secretions are drained into the nasopharinx[1,2].

The *nasal cavity* is formed by the nasal bones and separated into left and right halves by the nasal septum[17,18]. The *nasal septum* is easily identifiable both on coronal and axial tomographic sections. The anterior superior septum is composed of cartilage and the posterior portion is formed by bones, including the vomer and the perpendicular plate of the ethmoid bone (Figure 1)[3,17].

The nasal cavity lateral walls present several anatomical marks such as superior, middle and inferior nasal conchas, dividing the nasal cavity into three different air passages: the superior, middle and inferior meatuses (Figure 2A)[1,2,8,9].

The *superior nasal concha* is the smallest of the three conchas and forms the superior meatus below it, draining the posterior ethmoidal cells through the different ostia (Figure 2A). Above the superior concha, between the anterior wall of the sphenoidal sinus and the posterior wall of the ethmoidal sinus, is the sphenoethmoidal recess into which the sphenoidal sinus opens (Figure 5)[2,3,8,9].

The *middle nasal concha* covers the *middle meatus*, with the ostiomeatal unit (or complex) is the most complex region in the lateral wall of the nasal cavity, representing the final common pathway for drainage and ventilation of the frontal and maxillary sinuses and the anterior and middle third of the ethmoidal sinuses (Figures 2A and 2B)[1–9,17,19].

Anteriorly, the middle nasal concha is adjacent to the medial wall of the *agger*

---

* Study developed at Hospital Heliópolis Diagnostic Imaging Service, São Paulo, SP, Brazil.

1. Radiologist, Coordinator for Medical Residency in Diagnostic Imaging at Hospital Heliópolis, Doctor by Universidade de São Paulo.

2. Radiologist, Master Degree in Health Sciences at Hospital Heliópolis.

3. Radiologist, Master Degree in Health Sciences at Hospital Heliópolis, Professionalizing Practice in Magnetic Resonance Imaging at Universidade de São Paulo.

4. Radiologist, Doctor by Universidade de São Paulo.

5. Radiologist, Doctor Student at Universidade de São Paulo.

6. Radiotherapist, MD Assistant at Clínica Radium em Campinas and at Hospital das Clínicas da Faculdade de Medicina de Ribeirão Preto da Universidade de São Paulo.

7. Surgeon, Chief at the Service of Head & Neck at Hospital Heliópolis, Doctor by Universidade Federal de São Paulo.

Mailing address: Dr. Ricardo Pires de Souza. Rua Cônego Xavier, 276, 10º andar, Bairro Sacomã. São Paulo, SP, Brazil 04231-010. E-mail: ricapires@ig.com.br

Received October 28, 2004. Accepted after revision December 15, 2004.

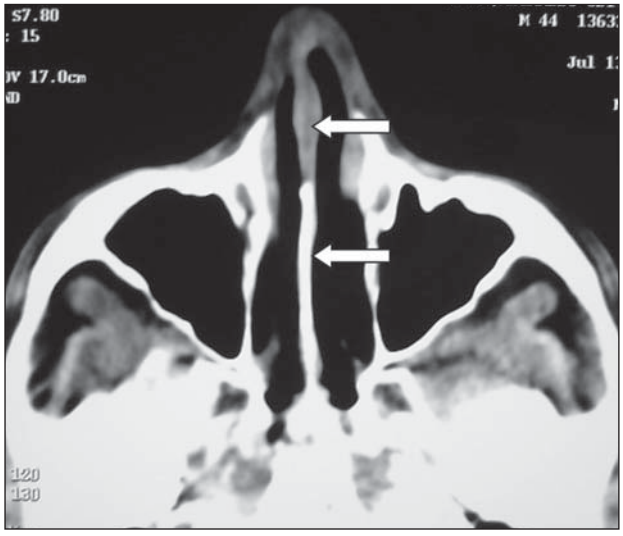

Figure 1. Axial CT image shows the anterior cartilaginous and posterior osseous portions of the nasal septum (arrows).

nasi cell and to the upper extremity of the uncinate process. Superiorly, it is attached to the cribriform lamina and posteriorly is fixed to the lateral wall of the nasal cavity through the *ground lamella* (Figure 5). The ground lamella is a lateral bony extent of the middle nasal concha which fuses to the lamina papyracea — a thin, smooth, oblong plate which covers in the middle and posterior ethmoidal cells and forms a large part of the medial wall of the orbit posteriorly to the ethmoid *bulla*[2,3,8,9].

The *uncinate process* is a thin, mucosal-lined osseous prominence, with its superior free edge forming the semilunar hiatus that opens directly into the middle meatus. Anteriorly, it originates the posteromedial edge of the nasolacrimal duct. The *infundibulum* is situated laterally to the uncinate process, connecting the maxillary and ethmoidal sinuses ostia to the semilunar hiatus. The inferomedial orbital margin defines the lateral limit of the infundibulum (Figure 2B)[1–8].

The *semilunar hiatus* is superiorly involved by the ethmoid *bulla*, laterally by the orbit, inferiorly by the uncinate process and medially communicates with the middle meatus. Laterally and inferiorly, the semilunar hiatus communicates with the infundibulum. The ethmoid *bulla*, generally is formed by a single ethmoid air cell projecting inferomedially over the semilunar hiatus (Figures 2A and 2B)[1–8].

The inferior meatus is situated below the *inferior nasal concha*, the largest of the three conchas, receiving the drainage of the nasolacrimal duct which is seen on CT axial sections[1–3].

The major draining ostia of the paranasal sinuses are:

1. The ostiomeatal unity, draining the frontal, maxillary sinuses and anterior and middle third of the ethmoid sinuses, and including the frontal sinus ostium, frontal recess, maxillary sinus ostium, infundibulum, uncinate process, ethmoid *bulla* ethmoidal, semilunar hiatus, middle nasal concha nasal and meatus (Figures 2A and 2B).

2. The sphenoethmoidal recess drains only the posterior third of the bilateral ethmoid and the sphenoid sinuses (Figure 5)[1–9,17,18].

The nasal cycle is a physiological phenomenon where each side of the nose al-

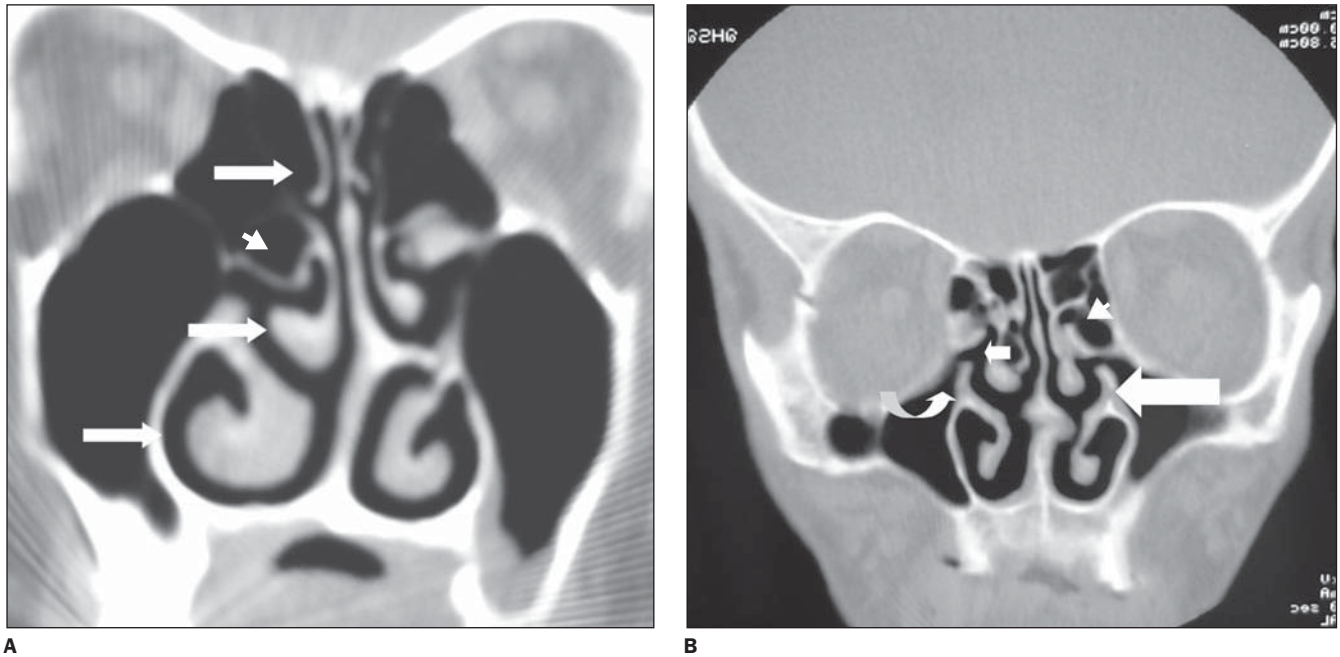

A **B**

Figure 2. A: Coronal CT image shows superior, middle and inferior nasal conchas (arrows) and ethmoid *bulla* (arrowhead). **B:** CT coronal section shows uncinate process (large arrow), infundibulum (curved arrow), semilunar hiatus (small arrow) and ethmoid *bulla* (arrowhead).

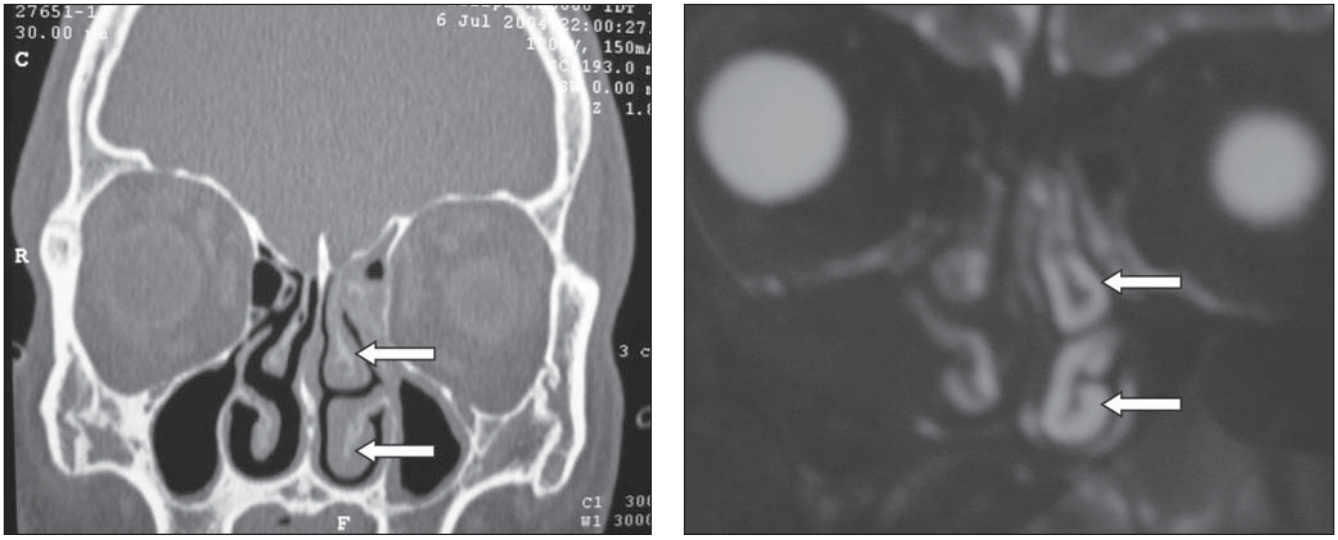

A B

Figure 3. A: Coronal CT image shows enlarged middle and inferior nasal conchas at left (arrows). **B:** Coronal, T2-weighted magnetic resonance image shows hyperintense enlarged middle and inferior nasal conchas at left (arrows). Such finding are considered as normal and attributed to the nasal cycle.

ternates through phases of congestion and decongestion. This cycle takes from 20 minutes to six hours to run and its control mechanism is still to be known (Figures 3A and 3B)[1,16,20,21].

MRI demonstrates such alterations through the increase in the signal intensity of the mucosal lining during the edematous phase of the nasal cycle, but this increase is quite similar to the appearance of a mucosal inflammation which usually presents hyperintense signal on T2-weighted sequences. On the other hand, neoplasms usually show intermediate intensity and fungal conditions present hypointense signal on T2-weighted sequences[1,12–14,22–24].

The *ethmoidal cells* are present at birth and continue to grow up to the puberty and usually are divided into three groups: the anterior, middle and posterior. The anterior ethmoidal cells usually drain through individual ostia opening into the infundibulum. The middle ethmoidal cells usually drain through the ethmoid *bulla*, or drain directly into the semilunar hiatus, or through the infundibulum and therefrom to the middle meatus via the semilunar hiatus. The posterior ethmoidal cells are those situated between the ground lamella and the sphenoidal sinus, draining into the superior meatus and, subsequently, into the sphenoethmoidal recess (Figure 5)[1,15,17,19,25].

The *frontal sinuses* vary in size and usually they are divided into left and right sides by a thin bony septum, although there may be other additional septa. They drain via the nasofrontal duct into the frontal recess, a narrowing between the frontal sinus and the anterior middle meatus, generally situated in the anterosuperior portion of the infundibulum, and continue through the semilunar hiatus towards the anterior portion of the middle meatus where it fuses to the flow of the ipsilateral maxillary sinus (Figure 4). Yet they may drain directly into the middle meatus, above the infundibulum[1,2,15,17,19,25].

The *sphenoidal sinuses* are the most posterior paranasal sinuses. Generally, they can extend as far as the clivus and are posterosuperiorly limited by the sella turcica. Their ostia are medially located in the anterosuperior portion of the anterior wall of each sinus, communicating with the sphenoethmoidal recess in the posterior portion of the superior meatus. The sphenoethmoidal recess is situated very laterally to the nasal septum and sometimes may be visualized on coronal sections although they may be better visualized on sagittal and axial sections (Figure 5)[1,15,17,19,25].

The *maxillary sinuses* are the first paranasal sinuses to develop and communicate with the middle meatus through the maxillary ostium and, subsequently, through the infundibulum and semilunar hiatus. They may extend laterally towards the zygoma and/or inferomedially towards the hard palate. Frequently, sinuses are asymmetrical in size and shape [1,15,17,19,25].

Anatomically, paranasal sinuses are in close contact with the anterior cranial fossa, the cribriform plate, the internal carotid arteries, the cavernous sinuses, the orbits and the optic nerves in their exit from the orbits[1].

ANATOMICAL VARIATIONS AND CONGENITAL ABNORMALITIES

Although the nasal anatomy presents many differences among individuals, certain anatomical variations are usually observed in the general population and most frequently are seen in patients presenting chronic inflammatory conditions. The relevance of a particular anatomical variation is determined by its relationship with the ostiomeatal channels and the nasal passages. Main variations are the following:

Variations of the middle nasal concha

• *Concha bullosa* – It is an aeration of the nasal concha, which may be uni or bilateral. The middle concha is most frequently affected and the middle meatus or infundibulum may be obstructed. Less frequently, aeration of the superior concha may occur, while in the inferior concha it is not frequent. Concha bullosa also may include polyps, cysts, pyoceles or mucoceles (Figure 6A).

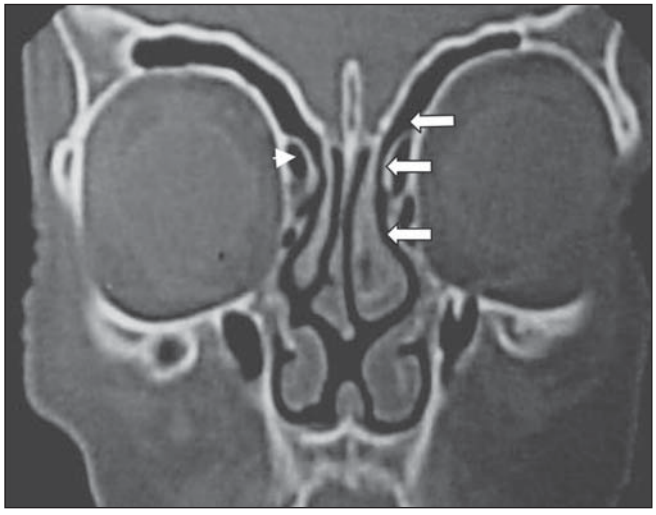

Figure 4. Coronal CT image shows the frontal recess (arrows) and *agger nasi* cell (arrowhead).

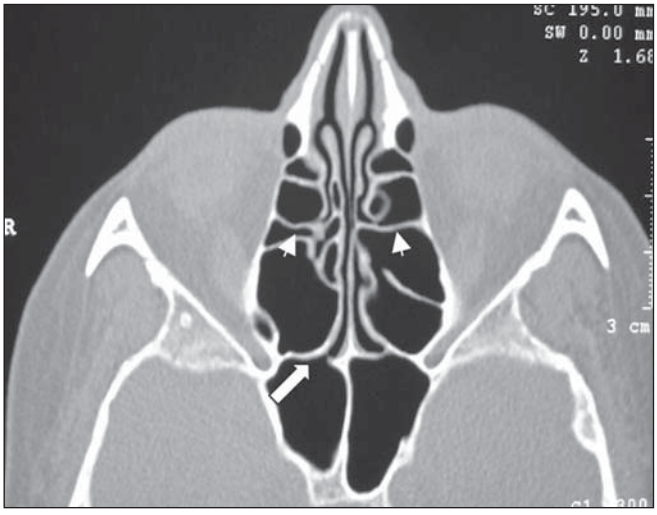

Figure 5. Axial CT image shows sphenoethmoidal recess (arrow) and ground lamella (arrowheads).

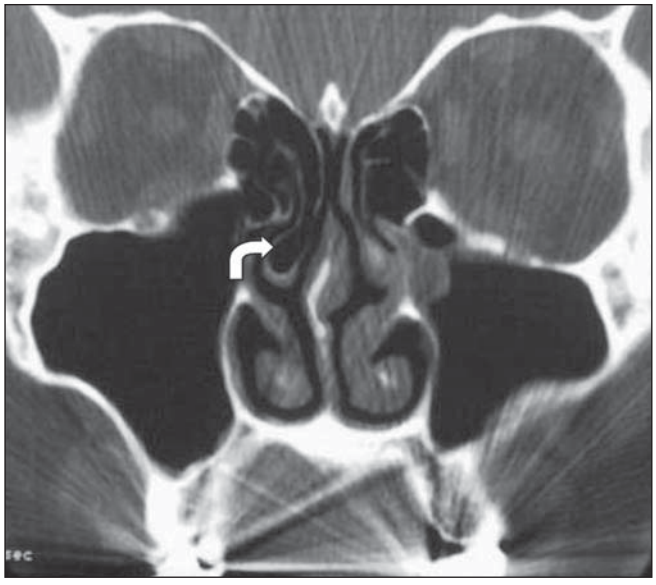

A

B

Figure 6. A: Coronal CT image shows middle concha bullosa (curved arrow). **B:** Coronal CT image bilaterally shows middle paradoxical concha (arrows).

• *Middle paradoxical concha* – Generally, the middle concha buckles and folds inward, with the resultant curve pointing toward the septum, but its major curvature may project toward the lateral sinus wall, narrowing the middle meatus and the infundibulum — this variation is called middle paradoxical concha (Figure 6B).

Uncinate process variations

• The uncinate process may present medial deviation, affecting the middle meatus, or lateral deviation, obstructing the semilunar hiatus and/or infundibulum.

• Less frequently, spiraling of the uncinate process may occur, obstructing the middle meatus.

• The uncinate process tip may fuse to the orbital floor or to the inferior portion of the lamina papyracea which is known as *atelectatic uncinate process* — this variation usually is associated with hypoplastic maxillary sinus, usually presenting ipsilateral opacification due to the closure of the infundibulum.

• Aeration of the uncinate – This anomaly expands the width of the uncinate, thus potentially compromising the infundibulum. Functionally, it acts as a concha bullosa or enlarged ethmoid *bulla*. It is not a frequent anomaly.

Ethmoid variations

• Haller air cells – They occur along the inferomedial orbital wall, in the region of the maxillary sinuses ostia and may vary in aspect and size and, when expanded, may cause narrowing of the infundibulum.

• Giant ethmoid *bulla* – The giant ethmoid *bulla* may be extremely pneumatized, narrowing or obstructing the middle meatus and/or infundibulum.

• *Agger nasi* cells – They are the most frequent ethmoid air cells, situated below the frontal sinus, inferolaterally to the lacrimal sinus, and represent pneumatization of the lacrimal bone through the extent of anterior ethmoid cells (Figure 4). They are situated anteriorly and superiorly to the middle nasal concha insertion, along the lateral nasal wall.

Hyperpneumatrization of the sphenoidal sinus – The pneumatization of the sphenoidal sinus may extend into the anterior clinoid processes and towards the clivus, involving the optic nerves. In these cases, the optic nerves present an increased risk of surgical damage (Figure 7).

Medial protrusion of the lamina papyracea – It may be a congenital finding or a result of a previous facial trauma. In this case, the intra-orbital contents are at risk during the surgical procedure.

Nasal septal deviation – It is an asymmetrical curve that may ipsilaterally compress the middle nasal concha, narrowing the middle meatus, possibly progress to secondary inflammation and infection (Figure 8)[1–4].

IMAGING METHODS

The purpose of the radiological evaluation of paranasal sinuses and related structures is to achieve the most possible precise description of the regional anatomy and to determine the presence and extent of a condition[1,22].

Plain films are widely available, however they pose very little use in surgical planning [1,3,22].

MRI allows an excellent visualization of soft tissues, but bone walls and paranasal sinuses ostia are not adequately demonstrated[11,12,22].

CT provides the most useful surgical information both on bone and soft tissues, remaining as the method of choice for evaluation of the presence or extent of conditions in paranasal sinuses. Coronal, 3-5mm thick slices, perpendicular to the hard palate, allow an optimal visualization of the ostiomeatal complex, besides simulating the plane seen by the endoscopist. CT scans are performed with the patient in prone position with his/her head fully extended in order to allow that the fluid is deposited on the maxillary sinus floor, avoiding a false obliteration of the ostiomeatal complex[1,3,6,22].

REFERENCES

1. Zinreich SJ. Functional anatomy and computed tomography imaging of the paranasal sinuses. Am J Med Sci 1998;361:2–12.
2. Mafee MF. Endoscopic sinus surgery: role of the radiologist. AJNR Am J Neuroradiol 1991;12: 855–860.
3. Laine FJ, Smoker WRK. Osteomeatal unit and endoscopic surgery: anatomy, variations, and imaging findings in inflammatory diseases. AJR Am J Roentgenol 1992;159:849–857.
4. Bolger WE, Butzin CA, Parsons DS. Paranasal sinus bony anatomic variations and mucosal abnormalities: CT analysis for endoscopic sinus surgery. Laryngoscope 1991;101:56–64.
5. Kennedy DW, Zinreich J, Rosenbaum AE, Johns ME. Functional endoscopic sinus surgery. Arch Otolaryngol 1985;111:576–582.
6. Babbel R, Harnsberger HR, Nelson B, Sonkens J, Hunt S. Optimization of techniques in screening CT of the sinuses. AJNR Am J Neuroradiol 1991;12:849–854.
7. Zinreich SJ, Kennedy DW, Rosenbaum AE, Gayler BW, Kumar AJ, Stammberger H. Paranasal sinuses: CT imaging requirements for endoscopic surgery. Radiology 1987;163:769–775.
8. Nayak SR, Kirtane MV, Ingle MV. Functional endoscopic surgery – I (anatomy, diagnosis, evaluation and technique). J Postgrad Med 1990; 37:27–30.
9. Nayak SR, Kirtane MV, Ingle MV. Functional endoscopic surgery – II (a preliminary study). J Postgrad Med 1990;37:31–34.
10. Babbel RW, Harnsberger HR, Sonkens J, Hunt S. Recurring patterns of inflammatory sinonasal disease demonstrated on screening sinus CT. AJNR Am J Neuroradiol 1992;13:903–912.
11. Shapiro MD, Som PM. MRI of the paranasal sinuses and nasal cavity. Radiol Clin North Am 1989;27:447–475.
12. Som PM, Shapiro MD, Biller HF, Sasaki C, Lawson W. Sinonasal tumors and inflammatory tissues: differentiation with MR imaging. Radiology 1988;167:803–808.
13. Dillon WP, Som PM, Fullerton GD. Hypointense MR signal in chronically inspissated sinonasal secretions. Radiology 1990;174:73–78.
14. Som PM, Dillon WP, Fullerton GD, Zimmerman RA, Rajagopalan B, Maron Z. Chronically obstructed sinonasal secretions: observations on T1 and T2 shortening. Radiology 1989;172:515–520.
15. Scuderi AJ, Harnsberger HR, Boyer RS. Pneumatization of the paranasal sinuses: normal features of the importance to the accurate interpretation of the CT scans and MR images. AJR Am J Roentgenol 1993;160:1101–1104.
16. Shankar L, Evans K, Halwke M, Stammberger H. An atlas of imaging of the paranasal sinuses. Philadelphia: JB Lippincott, 1995.
17. Babbel RW, Harnsberger HR. A contemporary

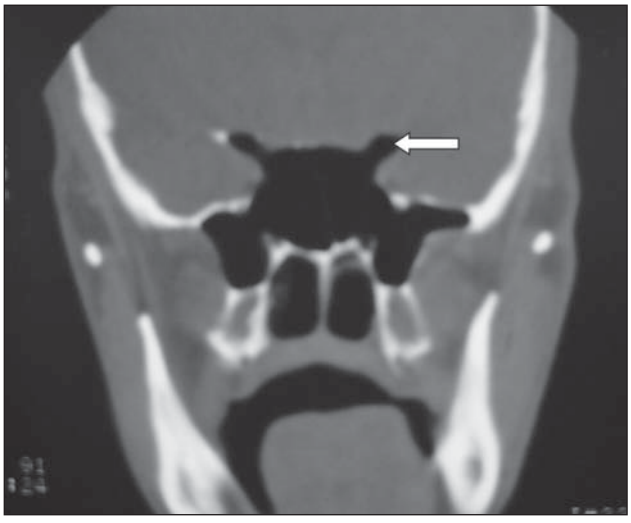

Figure 7. Coronal CT image demonstrating extensive pneumatization of the sphenoidal sinus and anterior clinoid process (arrow).

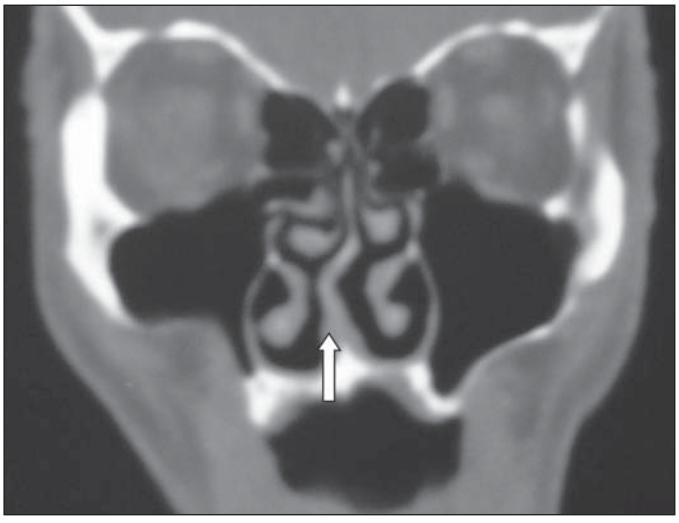

Figure 8. Coronal CT image demonstrating nasal septal deviation.

look at the imaging issues of sinusitis: sinonasal anatomy, physiology, and computed tomography techniques. Semin Ultrasound CT MR 1991;12: 526–540.

18. Osborn AG, McIff EB. Computed tomography of the nose. Head Neck Surg 1982;4:182–199.
19. Harnsberger HR, Babbel RW, Davis WL. The major obstructive inflammatory patterns of the sinonasal region seen on screening sinus computed tomography. Semin Ultrasound CT MR 1991;12:541–560.
20. Silva MB. L'imagerie IRM des pathologies inflammatoires et infectieuses des sinus de la face. Paris: Université Paris-SUD, 1992.
21. Doyon D. Pathologie des sinus de la face. Polycopie D.U. Maxillo-facial 1992;10–18.
22. Mafee MF. Modern imaging of paranasal sinuses and the role of limited sinus computerized tomography; considerations of time, cost and radiation. Ear Nose Throat J 1994;73: 532–542.
23. Zinreich SJ, Kennedy DW, Kumar AJ, *et al*. MR imaging of the normal nasal cycle: comparison with sinus pathology. J Comput Assist Tomogr 1988;12:1014–1019.
24. Terrier F, Weber W, Ruefenacht D, Porcellini B. Anatomy of the ethmoid: CT, endoscopic, and macroscopic. AJR Am J Roentgenol 1985;144: 493–500.
25. Aoki S, Dillon WP, Barkovich AJJ, Norman D. Marrow conversion before pneumatization of the sphenoid sinus: assessment with MR imaging. Radiology 1989;172:373–375.